An Autonomous Search for Moons during Approach of the *NEAR* Spacecraft to Asteroid Eros

W.J. Merline[1], P. Tamblyn[1,2], C.R. Chapman[1], W.B. Colwell[1], V. Gor[3], M.C. Burl[3], & E.B. Bierhaus[1]

ABSTRACT

We describe the first complete systematic search for natural satellites of an asteroid, conducted in near-real-time with automated software during the Near-Earth Asteroid Rendezvous (*NEAR*) spacecraft's approach to asteroid Eros. In addition to providing a unique scientific result, this points the way towards on-board autonomous systems for asteroid- or comet-approaching spacecraft. These systems could improve mission safety, operations, and value during critical events such as an approach or fly-by when light travel lags exceed event duration.

Four separate searches were conducted during the spacecraft's flyby and (1 year later) approach to orbit insertion around Eros. The automated search of the largest and most detailed image mosaic was completed within a few hours of data downlink. This mosaic imaged $\sim$ 95% of the volume in which a satellite could exist. The search for unidentified objects reached an approximate limit (95% confidence) of V-magnitude +5.0, corresponding to an object of approximate diameter 20 m. At diameter 10 m (V-magnitude 6.5), we would have about 70% confidence in our result. No unambiguous evidence for satellites was found.

Subject headings: Asteroids, Autonomous, Decision-Making, Hazard-detection, Imaging, Moons, NEAR, Real-time, Satellites, Spacecraft

1. Introduction

Although spacecraft are routinely empowered to respond autonomously to spacecraft safety threats, such as over-temperature or over-voltage conditions, they have always flown "blind" to scientific opportunities. Any action has to await transmission of data to the ground, human analysis, a human decision-making process, and transmission of commands back to the craft. Light travel time alone precludes real-time decision making. For example, the flyby of asteroid Mathilde by the NEAR-Earth Asteroid Rendezvous (*NEAR*) spacecraft lasted 25 minutes when the round-trip signal travel time to Earth was 36 minutes. The discovery of a moon (Dactyl) orbiting asteroid Ida from the *Galileo* spacecraft flyby data actually occurred months after the data were taken because the images trickled back to Earth through the low-gain antenna. With the existing ground-loop, there was obviously no opportunity in either of these two cases to retarget to get more images or spectra of an unexpected object. For Ida/Dactyl, many images were fortuitously acquired, but they were insufficient to determine, for example, the orbital parameters of the moon. Dactyl was actually discovered in the approach images, demonstrating the need for autonomous systems to detect scientifically-interesting features such as moons or debris, terrain boundaries, craters, morphological changes in comets, or spectral features. We are developing a functional framework in which these features can trigger redirection of mission activities to maximize scientific value during unique opportunities.

2. Asteroid Satellites

Detection of asteroid satellites is a particularly important application of autonomous software. In addition to mission safety (collision avoidance) and mission operations (trajectory perturbation) issues, satellite detection will yield a number of scientifically important results. The orbital characteristics of a satellite will provide an estimate for the mass of the primary asteroid. This will allow us to set limits of the asteroid's density and composition, and allow us to evaluate various theories for formation of satellites. The size, orbital parameters, and

[1]Southwest Research Institute *LastName@boulder.swri.edu*

[2]Binary Astronomy, LLC *LastName@astro101.com*

[3]Jet Propulsion Laboratory *LastName@aig.jpl.nasa.gov*

composition of a satellite hold significant clues to the origin and age of the asteroid itself and have larger implications for understanding asteroids as a whole, and consequently their role in the evolution of our solar system.

Asteroid satellites are almost certainly formed by collisions. One need only look at the cratered surfaces of solid bodies of the solar system or look to the leading theory of formation of our own Moon to know the importance of collisions to our history. An object's density is perhaps the single observable (not only of asteroids, but of anything) that is most fundamental in furthering our understanding of a body.

Until recently, ground-based searches for asteroid satellites have been hampered by lack of adequate spatial resolution to detect separations of fractions of an arcsecond and by lack of sufficient dynamic range of detectors to detect brightness differences of many magnitudes. The discovery of Dactyl during the 1993 flyby of Ida by the *Galileo* spacecraft(1; 2) showed that satellites can exist. Since that time, new results from ground-based adaptive optics imaging have uncovered additional asteroid companions, around 45 Eugenia, 762 Pulcova, 90 Antiope, and 87 Sylvia(3; 4; 5; 6). Evidence for binarity among the Near-Earth asteroid population is also accumulating. These discoveries show that Dactyl was not a fluke and it is worthwhile to search for moons during spacecraft encounters with asteroids. Non-automated searches for satellites during *NEAR*'s flybys of Mathilde and Eros are described in (7; 8)

3. Eros, *NEAR*, MSI, and Satellite Search Mosaics

The Near-Earth Asteroid Rendezvous (*NEAR*) mission was launched in February 1996 as the first of NASA's *Discovery* missions. After a flyby of asteroid Mathilde in June 1997, it proceeded to fly past, orbit, and eventually land on asteroid Eros. This is the largest asteroid with an orbit which approaches Earth's, making it more accessible to spacecraft and a representative of the class of asteroids relatively likely to impact the Earth. A premature burn shutdown before the originally scheduled orbit insertion led *NEAR* to speed past Eros in December 1998. Our first satellite search used images from both the approach and retreat phases of this flyby(8) (Figure 1). During the successful orbit approach in January and February 2000, three image mosaics were taken for dedicated satellite searches 33, 17, and 4 days prior to insertion. The corresponding ranges to Eros were 45000, 9000, and 4000 km. The most complete search (range 4000 km) consisted of over 300 images, taken in an 8x13 mosaic of tiles, spanning +/- 100 asteroid radii (a 20x20 degree patch of sky), and covering the gravitational sphere of influence of Eros.

All the flyby and approach images were taken with the Multi-Spectral Imager. This camera, described in detail in (9), has a 2.9x2.26 degree field of view projected onto a 537x244 pixel 12-bit frame transfer Si CCD. The broadband filter used for the search mosaics has a central wavelength of 700 nm and a width of $\sim$ 200 nm. Maximum exposure time is limited by the camera to one second.

4. Automated Satellite Detection

4.1. Broad Technique

The *DARE* tool (10) forms the procedural basis for our automated satellite detection. This is a general tool applicable to a range of detector, image, and relative motion characteristics. *DARE* leverages predictable motion, projected onto the image plane, to identify and track satellite candidates from a temporal sequence of images. It distinguishes them from similar-appearing features such as background stars, detector defects, and cosmic ray events. The steps involved are summarized in Table 1. With each image, sources are detected after a detector-specific pre-processing stage that removes static artifacts such as flat-field response. Region segmentation links pixels brighter than the background. The resulting regions are reduced to characterizations such as position, size, brightness, and compactness. The registration step uses the spacecraft quaternion and matches identified sources with catalogued stars in the field. The region list is pruned of known objects and detector defects.

4.2. Early Tests

Our initial tests of automated software were made using ground-based telescopic data, which consisted of particularly sharp adaptive-optics images of asteroids. These sharp images were very similar to those what would be taken by a spacecraft on approach to an asteroid. In addition, we tested the algorithms on spacecraft images of Ida taken many years before by the *Galileo* spacecraft, and containing images of Dactyl. Thus, the software could be trained on actual data, including associated problems of detector defects, radiation noise, image pattern noise, inherent photon and background noise, and changes in perspective during a spacecraft flyby.

The problem with these tests is that they lacked the urgency associated with a real-time demonstration. To do this, we made use of our positions as Team Members of the Imaging and Infrared Spectrometer Teams on the *NEAR* Mission. We were able to employ the software in an actual search for satellites from real-time spacecraft data, with real scientific objectives and deadlines. A trial run of the software was made in December 1999, when *NEAR* made a close flyby of asteroid Eros en route to its eventual rendezvous and orbit a year later.

4.3. Tests with *NEAR*

In the case of *NEAR*'s orbital approach, a ground-loop search by humans for companions was required for mission safety. Hence, the satellite search image sequences were all made at $\geq$ 4000 km distance. At this distance, the geometrical flexibility of the *DARE* system was unimportant as Eros' entire sphere of gravitational domination subtended a small angle. Also, temporal extent of the search was too small to show much satellite orbital motion or parallax. Hence, our emphasis during these tests was on the candidate detection, image registration, and candidate verification. These tasks were broken out and optimized for the expected data stream. Data from earlier in the mission were used with synthetic data for this optimization.

4.4. *NEAR*-specific Preprocessing and Candidate Detection

The camera used has several unusal traits relevant to this experiment. Briefly, the pixels are rectangular with an aspect ratio of 1.7:1; this results in a marked X-Y asymmetry in the point spread function. Synthetic data were used to develop a point detection filter optimized for this pixel geometry. Second, alternate scan lines have significantly different sensitivities. We compensated for this by accepting a limiting brightness sufficient to be unambiguously seen in the less sensitive lines and accepting generous uncertainties in all derived candidate centers. Third, the images have an artifact of electronics crosstalk. This could be effectively removed with a Fourier filter developed from examination of data taken earlier in the mission. Fourth, bright objects off-frame can bleed through the "opaque" covering on the storage area of the detector during readout. We intentionally did not compensate for this but left it as a realistic challenge to the software. These pre-filtering steps were well understood before the approach sequence and were not further modified or optimized.

The satellite search images were automatically preprocessed and then independently searched for candidate objects. These are local peaks in the convolution of the image with a filter matching a slightly smoothed expected point spread function. The images from the 1998 flyby conclusively ruled out a large companion, so any object in the detailed search mosaics was expected to subtend at most a couple pixels, even in the mosaic with the closest range.

4.5. Rejection of Detector Artifacts

With a reasonable threshold such as 2 sigma above the noise limits, the initial candidate list has many thousands of entries across the image mosaic. Each search mosaic was treated independently. The primary challenge to the automated search is to reject candidates arising from image artifacts, radiation events, and known astronomical (distant) objects such as background stars. As mentioned above, no real orbital motion or projection of spacecraft parallax is expected in the data. Hence, candidates are expected to move in the images with the star field due to continuous spacecraft slew. This motion is sufficient in the flyby images to distinguish clearly stars and candidates from hot or unreliable (warm) pixels in the detector array. However, in many of the image pairs in the orbit approach mosaics (at the mosaic edges), the projected slew is less than 2 pixels. Hence, motion alone could not be used to distinguish candidates from detector flaws. Instead, a list of flaws was generated from earlier data and all candidates within 2 pixels were rejected. A better approach would be to construct the imaging sequence without images at the slew turnaround points.

4.6. Registration and Rejection of Distant Astronomical Objects and Radiation Events

The positions of surviving candidates are then mapped from image to astronomical coordinates. An initial transformation is conducted based on the spacecraft quaternion. Bright stars expected to be in the image field are then compared with the list of candidates to improve the registration and final tranformations are performed. We expected to perform this step on each image independently, but found in the first approach sequence that some fields had too few bright stars. So for the subsequent searches, the entire mosaic was used to determine a global quaternion correction.

Surviving candidates are then compared to star catalogs to reject stars expected to be sufficiently bright in the red. The camera has a maximum exposure time of 1s, so the broadest filter was used for the satellite search to maximize signal. Unfortunately, no star catalog is a good proxy for the resulting sensitivity function. We used $m_V - (m_B - m_V)$ as a coarse approximation. This resulted in the automated search returning 3 candidates which were actually very cool stars. One could easily construct a better approximation for the expected brightness, but a star catalog matched to the observed wavelength would be preferred. A typical image included 5 – 20 stars listed in our primary catalog (SAO) and also included fainter red stars for which deeper catalogs were used.

Random radiation events are eliminated by requiring a candidate to appear brighter than a set threshold in at least 2 images. All regions of the search mosaics were imaged at least 3 times. The mosaic tiles overlap, frequently allowing 6 to 9 detections of real astronomical sources. We were limited by downlink resources — in a real autonomous search with sufficient on-board processing resources, one would want to reimage repeatedly and require several consistent detections.

4.7. *NEAR* Test Results

The initial flyby and first two approach mosaics were mostly used to continually refine our automation in anticipation of the final mosaic which was by far the largest and most likely to have a detectable object. These 3 preliminary searches were vital to setting up for a fully automated final search. For example, we learned that the coordinate system stored in the image headers changed between the flyby and first approach sequence and the data were not timestamped in the manner we had originally anticipated. This final mosaic search was completed within a few hours of acquiring the data. We reached an approximate limit (95% confidence) of V-magnitude +5.0, corresponding to an object of approximate diameter of 20 m. At diameter 10 m (V-magnitude 6.5), we would have about 70% confidence in our result. No unambiguous evidence for satellites was found.

Approximately 5,000 background stars were automatically identified and rejected. The final candidate list did include what subsequent analysis revealed to be several very cool stars whose brightnesses were poorly predicted by our ad-hoc star catalog. There were also many reported candidates in the glare immediately surrounding Eros. This is due to scattering, substantially stronger than in early mission data, presumably from propellant residue which deposited on the camera lens during *NEAR*'s 1998 control anamoly. Figure 3 shows this obstacle. Finally, the known bleed-through when Eros was illuminating the storage portion of the chip resulted in a ghost image which was repeatedly flagged by the software as a candidate. As mentioned above, we intentionally did not correct for this image artifact to see if the software would identify it.

This test differed from a complete feasibility demonstration in two ways of consequence. First, the computing resources used (a Sun Ultra 5 with sufficient disk to hold complete star catalogs) greatly exceed those currently on-board spacecraft. Second, although the satellite search was a mission priority, making it appropriate for an automated search was not. Hence, for example, the search image sequences were rescheduled and compressed, invalidating some of our anticipations such as the background star field and slew pattern. Nor could we obtain as many repeat images per field as would be appropriate for an automated search.

5. Results

As a result of this experiment, confirmed by the manual search done in parallel, Eros is the first asteroid known not to have a companion larger than about 20 m (95% confidence). The automated search showed that a real-time autonomous search for small unexpected bodies is practical during approach. In contrast, the manual search was not completed until weeks later. A companion search would be a valuable element in the approach to any small body in the solar system both for mission safety and to allow for retargetting to obtain high value science observations. A search conducted on-board has the greatest scientific value because of downlink restrictions and light travel time delays.

References

[1] **Belton's Dactyl Reference**

[2] **Chapman Reference**

[3] Merline *et al.* 1999, Nature **401**, 565-568

[4] Merline *et al.* 2000, BAAS **32**, 1309

[5] **Antiope Reference**

[6] Brown & Margot 2001

[7] Merline *et al.* LPSC **Mathilde Search Reference**

[8] Merline *et al.* 1999, LPSC **30**, 2055

[9] Veverka *et al.* 1997, JGR **102**, 23709

[10] Gor *et al.* 1999, AIAA

Table 1: *DARE* Process Elements

#	Task	Purpose
1	Preprocess	Enhance object contrast in image
2	Detect	Locate objects, stars, etc.
3	Characterize	Reduce objects to size, position, etc.
4	Register	Remove jitter, slew
5	Static Rejection	Remove stars, detector defects, etc.
6	Coincidence	Link related detections
7	2-D Track Comparison	Reject random events, cosmic rays; require track coherence
8	3-D Track Projection	Adjust track predictions for parallax
9	Report	Report candidates to scientists
10	Follow-up	Select follow-up observation

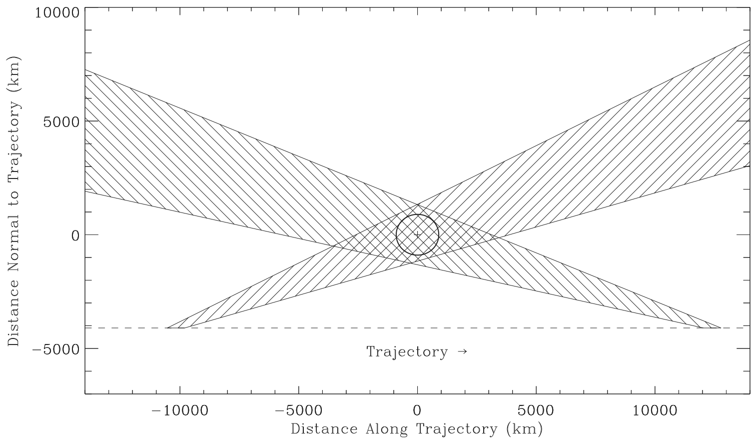

Fig. 1.— Image mosaics taken during both approach and retreat of the 1998 flyby covered the entire volume within which satellites of Eros can exist during both approach and retreat. This view is from above the plane of the spacecraft trajectory and asteroid.

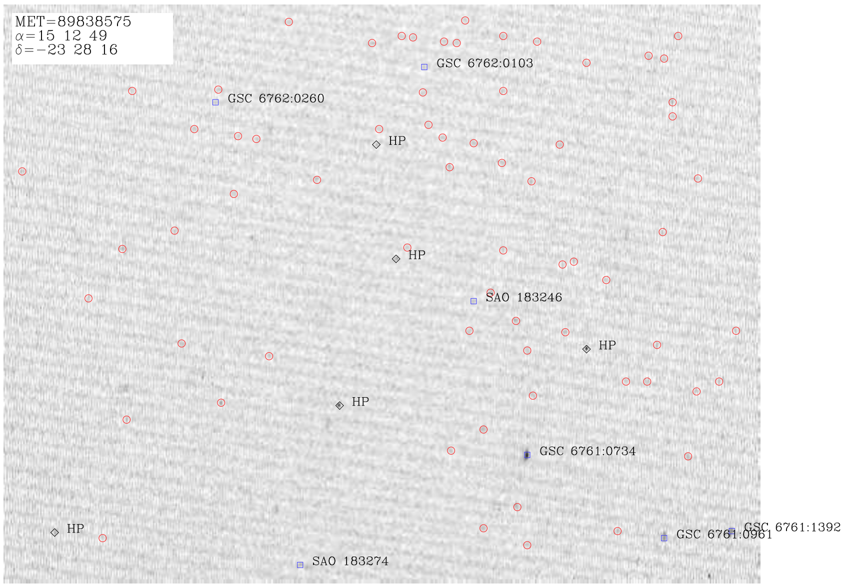

Fig. 2.— This is a "negative" image (bright objects are dark in the picture) taken during the flyby on December 23, 1998. The asteroid is off the field of view of this image, taken to look for nearby faint companions. Several characteristic image features are marked: defective pixels (HP) in diamonds, known stars in squares are labelled with their catalogue identifiers (SAO # or GSC #), and potential objects are circled. By requiring persistence from one image to the next, we next eliminate cosmic ray hits and random image noise. The banding is a correctable electronics artifact.

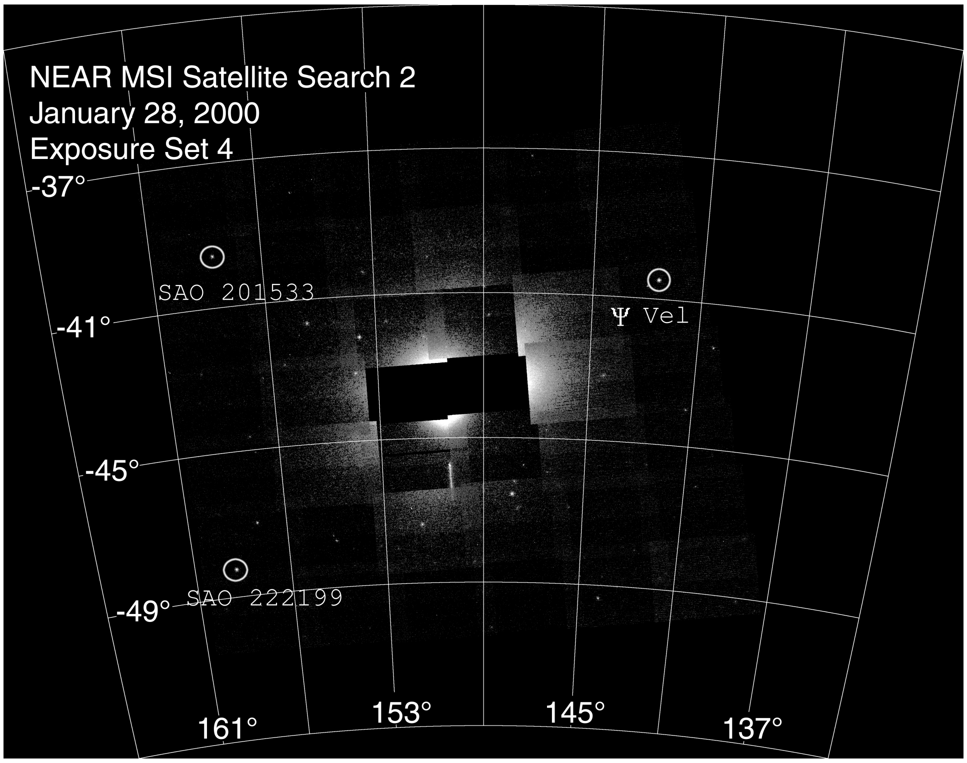

Fig. 3.— The whole area of the smallest satellite search image mosaic taken during orbit approach is shown. 500 background stars were automatically identified from these 129 images of 42 fields. Several bright stars are labelled here. Eros itself was pintentionally avoided, leaving the two empty frames near the center. Glare and scattered light from Eros dominates all but the brightest stars over the central 2 degrees.